IEEE Access
Multidisciplinary | Rapid Review | Open Access Journal

Received September 27, 2020, accepted October 24, 2020, date of publication November 5, 2020,
date of current version December 7, 2020.

Digital Object Identifier 10.1109/ACCESS.2020.3036128

Dynamic Monitoring and Analysis of Land-Use and Land-Cover Change Using Landsat Multitemporal Data in the Zhoushan Archipelago, China

CHAO CHEN[1,4], (Associate Member, IEEE), HUIXIN CHEN[1], WEIMIN LIAO[2], XINXIN SUI[3], LIYAN WANG[1], JIANYU CHEN[4], AND YANLI CHU[5]

[1]Marine Science and Technology College, Zhejiang Ocean University, Zhoushan 316022, China
[2]Zhoushan Natural Resources Surveying and Mapping Design Centre, Zhoushan 316000, China
[3]Land Satellite Remote Sensing Application Center, Ministry of Natural Resources, Beijing 100048, China
[4]State Key Laboratory of Satellite Ocean Environment Dynamics, Second Institute of Oceanography, Ministry of Natural Resources, Hangzhou 310012, China
[5]School of Economics and Management, Zhejiang Ocean University, Zhoushan 316022, China

Corresponding author: Xinxin Sui (sxx5666@163.com)

This work was supported in part by the National Natural Science Foundation of China under Grant 41701447, in part by the Training Program of Excellent Master Thesis of Zhejiang Ocean University.

ABSTRACT Rapid urbanization, marked by massive land-use and land-cover change (LUCC) and explosive population growth, has a significant impact on human activities. To provide a comprehensive understanding of the characteristics of LUCC in the Zhoushan Archipelago, dynamic monitoring and analysis of LUCC was performed using seven Landsat images from 1984 to 2016. The observations and results obtained in this study include the following: the forest of Zhoushan Island was well protected and had a slight increase in the area, yet the spatial distribution remained nearly unchanged; the construction land gradually expanded to all of the coastal plains and southern islands with a trend ''first southward, then eastward and finally northward,'' and the area increased by 571.88%; the coastal cropland/grassland surrounding Zhoushan Island was observed to have been gradually occupied by construction land as noted by a 27.94% decrease in area and the spatial distribution becoming discrete; the mudflat decreased by 93.39% and was mainly converted into construction land; the total land area observed in this study increased by 8.87%, which was achieved primarily by sea reclamation and conversion to construction land and inland water body. These results provide a better understanding of the spatial and temporal evolvement features of LUCC in Zhoushan, China, and the LUCC characteristics that can be expected to significantly support urban management and sustainable development.

INDEX TERMS Zhoushan island, land-use and land-cover, spatial-temporal pattern, supervised classification, accuracy assessment.

I. INTRODUCTION

The land is the material foundation of city development, the demands of which are always exceeding the supply, so the sustainable use of land resources will be significantly helpful for the sustainable development of the regional economy [1]. Collection and updating of the land-use information are the basic tasks of land management, which also form the basis and foundation of scientific decision-making and planning of land resource use [2], [3]. Traditionally, land-use monitoring has been conducted by field survey and manual measurement; while this approach is highly accurate, it requires a lot of time and labor [4], [5]. Comparatively, remote sensing dynamic monitoring has clear advantages in timeliness, economy, and accuracy, and it has been widely used in resource management and land planning [4], [5]. Through the image superposition analysis method and the multidate classification method, remote sensing can be used to quickly obtain

The associate editor coordinating the review of this manuscript and approving it for publication was Marco Anisetti.

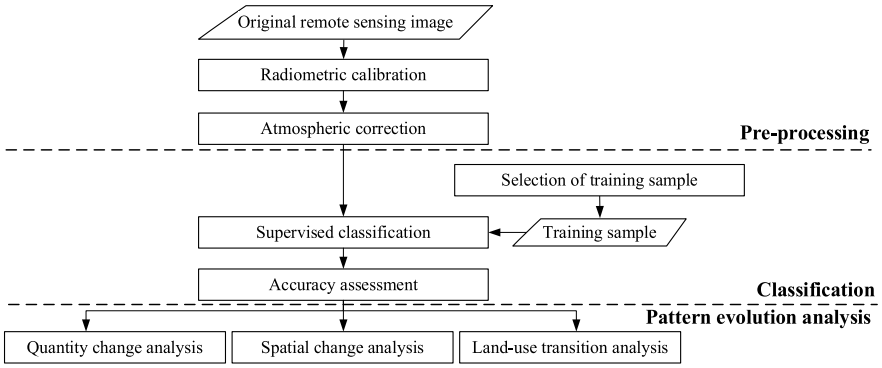

FIGURE 1. Flowchart of dynamic monitoring and analysis of land-use and land-cover using multitemporal remote sensing data.

land-use and land-cover (LUCC) information and update the land-use map; in fact, these methods have been widely used in land monitoring since the 1970s [6], [7].

Dynamic monitoring and analysis of LUCC based on remote sensing technology refer to the classification of multidate remote sensing images to obtain the land-use type and change information in a certain period for a study area [8]. With long time-series satellite images, remote sensing technology has been widely used in land-use monitoring by various regions in China and abroad [9], [10]. Internationally, the land-use changes of Dakaria in Egypt, a northern region in Rwanda, Nagadeh in Iran, metropolitan areas of Atlanta, Georgia, in the United States, and Hue City in Vietnam have been studied using remote sensing images obtained by satellites, such as Landsat (an Earth observation satellite commissioned by the U.S.) and SPOT (Satellite Pour l'Observation de la Terre, an Earth observation satellite initiated by France), [11]–[15]. In China, the dynamic changes of land-use in Beijing, Shanghai, Guangzhou, Jiaozuo, Wuyishan, and Jining have been monitored, and the land-use evolvement procedures of the Dongjiang River Basin, Pearl River Estuary, and Yellow River Delta have been analyzed [16]–[18].

The city of Zhoushan, China was established in 1987 and is the first prefecture-level city of the Zhoushan Archipelago; in 2011, the ''Zhoushan Archipelago New District'' was set up, which also became the first national strategic new district with the theme of the ocean economy [19], [20]. Zhoushan is mainly composed of islands surrounded by water, and its land area is small and scattered; in essence, land resources are few and insufficient here [7]. The establishment of a new district pushed Zhoushan's economy to grow rapidly, and the permanent population continuously increased. As a result, a noticeable conflict between supply and demand for land resources occurred. The island ecosystem has its own unique vulnerability, which is difficult to recover once it has been disturbed or destroyed [7]. However, there is little long time-series information about dynamic change in land-use for the Zhoushan Archipelago. Therefore, to provide the required information of LUCC, seven Landsat images of the Zhoushan Archipelago from 1984 to 2016 are classified in this study, and the spatial-temporal pattern of land-use in this period are analyzed for quantity change, space change, and change features. The study provides the spatial-temporal pattern of the evolving features of land-use in the Zhoushan Archipelago, and timely and accurate monitoring of island LUCC is of great significance for regional sustainable development.

II. METHODOLOGY

The dynamic monitoring and analysis of LUCC using multitemporal remote sensing images mainly include image pre-processing, image classification, and pattern evolution analysis. The flowchart is shown in Fig. 1.

A. REMOTE SENSING IMAGE PRE-PROCESSING

Remote sensing image pre-processing includes three parts: radiometric calibration, atmospheric correction, and image cropping. First, the digital quantizing value is converted into physical radiance value by calibration parameters. Then, the FLAASH, which stands for the ''fast line-of-sight atmospheric analysis of spectral hypercubes'' model is used for atmospheric correction to eliminate the radiance error caused by atmospheric absorption and scattering. Finally, the images are cropped according to the required research area to obtain the required images. As the research area is surrounded by sea and might expand from time to time, the cropped area will be slightly larger than the actual margin, including part of the sea outside of the border, which will be removed in post-processing to acquire the boundary change of the research area.

B. CLASSIFICATION

According to the characteristics of the study area, training samples are selected by the random sampling method, and supervised classification is carried out by the maximum likelihood method. The overall accuracy and Kappa coefficient are used to evaluate the accuracy of the classification results to determine the reliability of classification.

C. PATTERN EVOLUTION ANALYSIS

Based on multitemporal of land-use information obtained by remote sensing image classification, evolution analysis

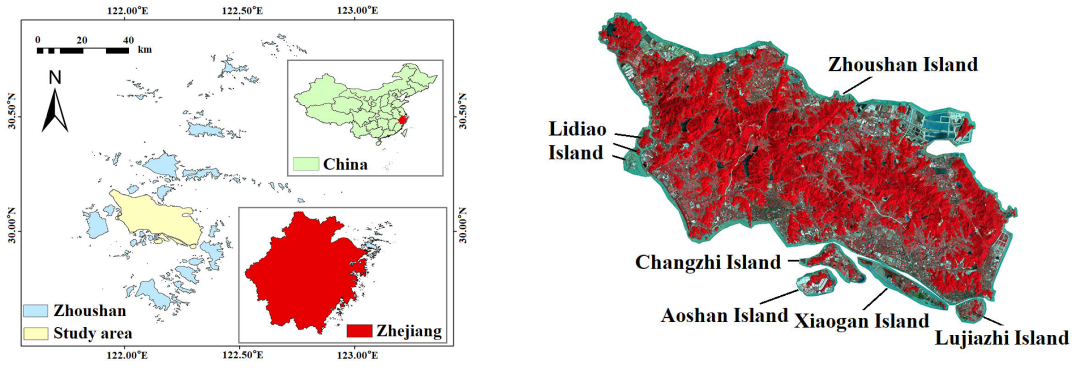

(a) The location of the study

(b) Pre-processed image of the study area (false color synthesis)

FIGURE 2. The study area.

of spatial-temporal pattern is performed from three perspectives: quantity change, spatial change, and land transition.

III. STUDY AREA AND DATA

A. STUDY AREA

The Zhoushan Archipelago consists of 1390 islands and is located on the east coast of the East China Sea, west of Hangzhou Bay, north of Shanghai, south of Ningbo, and east of the Pacific Ocean (Fig. 2). It is a maritime gateway and channel open to the Yangtze River Basin and the Yangtze River Delta, so it has substantial geographical advantages [7]. In terms of geographic spatial distribution, the archipelago belongs to the low mountain and hilly type of landform, with a large area, high altitude, and dense distribution in the south and a small area, flat terrain, and sparse distribution in the north. In terms of climate, the Zhoushan Archipelago has a monsoon marine climate in the southern margin of the northern subtropical zone with an average annual temperature of 16 °C [20]. The Zhoushan Archipelago is located at the intersection of the Yangtze, Qiantang, and Yong rivers, which bring to the archipelago a large amount of nutrients, which are conducive to the habitat and reproduction of various marine organisms.

The study area covers Zhoushan Island and its adjacent well-developed islands such as Changzhi Island, Aoshan Island, Xiaogan Island, Lujiazhi Island, and Diaoshan Island (inner, middle, and outer of Diaoshan Island). Zhoushan Island is the first large island in the Zhoushan Archipelago; it is the administration and economic center of the city of the Zhoushan Archipelago.

B. DATA

Landsat is a series of land satellites projected by the National Aeronautics and Space Administration, i.e., NASA, and is one of the optical remote sensing satellite series with the longest operational time in orbit. There have been eight satellites in total since 1972 [21]. Landsat5 with Thematic Mapper (TM) and Landsat8 with Operational Land Imager (OLI) were launched in 1984 and 2013, respectively, and the spatial resolution of their multispectral bands is 30 m, are particularly suitable for large-scale land-use monitoring [22], [23].

In the study, the original Landsat data is Level 1 Terrain Corrected (L1T) product, which is radiometrically corrected and co-registered to a cartographic projection, with corrections for terrain displacement resulting in a standard orthorectified digital image [24]–[26]. According to the current data source and the needs of this research study, seven images were selected, all with a cloud cover less than 5%. All images have perfect imaging effect and a time intervals of approximately 5 years. The total period is 32 years. The date each image was taken is shown in Table 1.

IV. RESULTS AND DISCUSSION

A. RESULTS OF LAND-USE CLASSIFICATION

The land-use type within the study area was first ascertained. Because numerous hills are scattered across the island, the spatial distribution of objects within the research area is quite dispersed. Limited by the spatial resolution, the land-use within the research area was integrated and classified into six types: construction land, forest, water body, cropland/grassland, bare land, and mudflat (Table 2).

The images pre-processed by radiometric calibration, atmospheric correction, and image cropping were classified by the supervised classification methods. First, the training sample was selected with a degree of separation above 1.8. Then, the samples were supervised and classified by the maximum likelihood method. Finally, the classified results were processed, and any classification that was clearly incorrect was manually modified. The results of the land-use classification are shown in Fig. 3.

Accuracy assessment is a crucial step to verify the classified results. Taking advantage of the historical imaging function of Google Earth, a new set of samples that were dated the same period were selected to assess accuracy. The average value of the overall accuracy and Kappa coefficient were 82.31% and 0.78, respectively (Table 3). The accuracy assessment showed that the land-use type in the study is accurately identified and the results of land-use classification

TABLE 1. Information of the Landsat satellite images used in the study.

Satellite	Imaging time	Sensor	Spatial resolution (m)	Product level
Landsat5	April 23, 1984	TM	30	Level 1 Terrain Corrected product
Landsat5	June 11, 1990	TM	30	
Landsat5	August 12, 1995	TM	30	
Landsat5	April 1, 1999	TM	30	
Landsat5	June 4, 2005	TM	30	
Landsat5	May 20, 2011	TM	30	
Landsat8	May 1, 2016	OLI	15 for panchromatic band 30 for multispectral band	

Note: TM and OLI refer to Thematic Mapper and Operational Land Imager, respectively.

TABLE 2. Land-use types classified in the study.

Type	Sub-type
Construction land	Urban and rural residents land, industry land, transportation, and water conservancy land
Forest	Trees, shrubs, orchards
Water body	Lake, river, reservoir, pond
Cropland/grassland	Crop, grassland
Bare land	Bare land, mountains without vegetation cover, land under construction
Mudflat	Tidal flat, salt land, aquaculture land

TABLE 3. Accuracy assessment of classification.

Year	Overall accuracy (%)	Kappa coefficient
1984	84.92	0.81
1990	76.58	0.71
1995	82.48	0.76
1999	87.05	0.84
2005	77.86	0.71
2011	83.80	0.81
2016	83.50	0.80
Average	82.31	0.78

TABLE 4. Area of various types of land-use.

Year	Construction land (km^2)	Forest (km^2)	Water body (km^2)	Cropland/grassland (km^2)	Bare land (km^2)	Mudflat (km^2)	Total (km^2)
1984	19.56	210.71	5.63	220.70	19.85	29.35	505.80
1990	26.89	200.24	5.00	204.39	42.47	25.06	504.05
1995	36.19	222.66	3.95	203.54	23.31	16.65	506.30
1999	50.03	217.79	7.73	207.31	8.23	15.77	506.86
2005	64.20	250.30	7.39	147.90	35.57	11.66	517.02
2011	98.72	226.82	6.03	178.11	15.91	6.05	531.63
2016	131.42	226.78	11.18	159.04	20.28	1.94	550.64

can be used for evolution analysis of the spatial-temporal pattern.

B. EVOLUTION ANALYSIS OF SPATIAL-TEMPORAL PATTERN

1) QUANTITY CHANGE ANALYSIS

The area of land-use types in different periods is shown in Table 4 and Fig. 4.

Within the timeframe of the research study, the area of construction land within the research area increased continuously, and the area of mudflat decreased continuously. There were also large variations in areas of cropland/grassland and forest, that is, the former decreased in general while the latter increased. The area of water body varied very little before the year 2011 but increased significantly afterward. Bare land appeared to increase first but later decreased. These changes are described in further detail as follows:

(1) The area of construction land continued to increase, which was presented mainly in two phases according to the growth rate: one from 1984 to 2005, during which the area of construction land expanded at a rate of 2.13 km^2 per year with an increase that reached 228.22% within 21 years; and

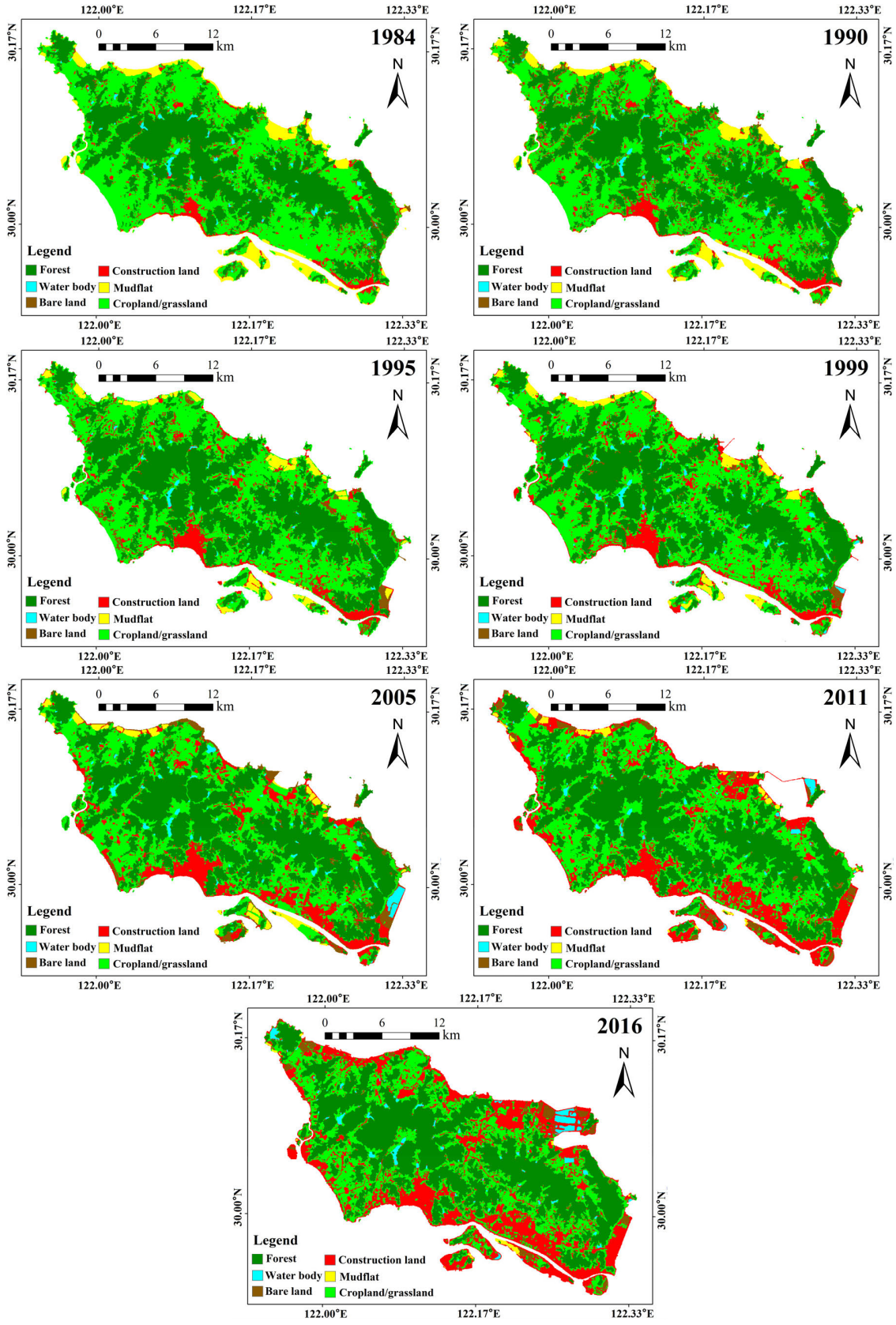

FIGURE 3. Results of land-use classification.

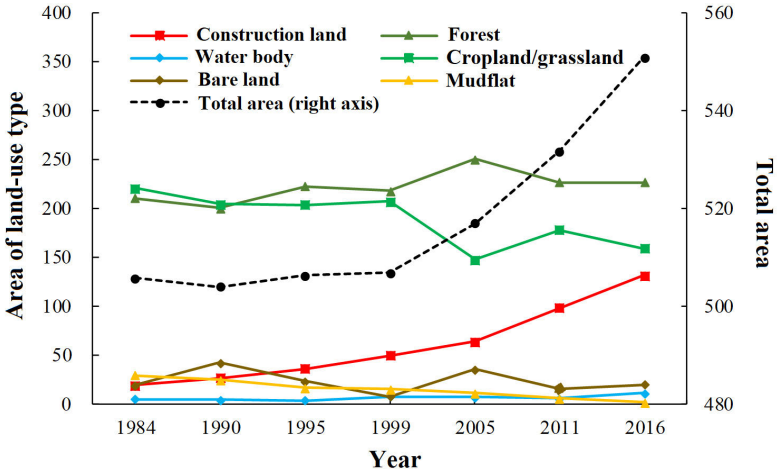

FIGURE 4. Area of land-use types from 1984 to 2016.

another from 2005 to 2016, during which it grew by 6.11 km^2 per year and increased by 104.70% in total within 11 years. Overall, the area of construction land increased by 571.8%, totaling 111.86 km^2; its annual growth rate was 3.50 km^2, and its annual change rate reached 17.8%.

(2) Fluctuation was observed in the area of the forest but increased as a whole. From 1984 to 2005, the area of the forest increased in a zigzag pattern by 39.59 km^2, corresponding to an increase of 18.7%. However, from 2005 to 2011, the forest decreased sharply by 9.3%, corresponding to a total area of 23.48 km^2. From 20011 to 2016, there was no apparent change. Overall, the area of the forest increased by 16.07 km^2, which was an increase 7.63% within 32 years, and the annual change rate was 0.20%.

(3) For the water body area, there were a few minor changes by the year 2011, and then it increased significantly afterward. Water body area increased by 5.15 km^2 from 2011 to 2016, an increase of 85.40%. Overall, the water body area increased by 5.55 km^2, an increase of 98.58% within 32 years; the annual change rate was 3.0%.

(4) Cropland/grassland showed fluctuation but decreased as a whole. It decreased by 16.31 km^2 from 1984 to 1990, corresponding to a 7.39% reduction; it had a comparatively stable increase of 2.92 km^2 in total from 1990 to 1999, which was an increase of 1.4%; the area of cropland/grassland decreased sharply, by 59.41 km^2 from 1999 to 2005, which was a decrease of 28.6%; and increased by 30.21 km^2 from 2005 to 2011, which was an increase of 20.43%, then decreased by 19.07 km^2, which was a decrease of 10.71%. In total, the cropland/grassland decreased by 61.66 km^2, which was a decrease of 27.94%, and the annual change rate was −0.87%.

(5) The area of bare land fluctuated significantly with a trend that first increased then decreased. It increased in three periods, that is, 1984–1990, 1999–2005, and 2011–2016 by 22.62 km^2, 27.34 km^2, and 4.37 km^2, respectively, with the respective rate of 113.96%, 332.20%, and 27.47%. It decreased in two periods, i.e., 1990–1999 and 2005–2011 by 34.24 km^2 and 19.66 km^2, respectively, with the respective rate of 80.62% and 55.27%. Therefore, the bare land increased by 0.43 km^2, up 2.17%, and the annual change rate was 0.07%.

(6) The area of mudflat continually decreased. It decreased by 27.41 km^2, which was a decrease of 93.39% within 32 years, and the annual change rate was −2.92%.

2) SPATIAL CHANGE ANALYSIS

The spatial distribution of ground objects in the seven periods is shown in Fig. 3. The key features of the spatial distribution of ground objects in the study area after comparison, analysis, and summary are as follows:

(1) The expansion of construction land along the seashore and cropland/grassland tended to be discrete. As shown in the classification results in 1984, two red dots representing the construction land appears in the southern coastal plain of Zhoushan Island and three small points in the northern interval. This expansion first started from the plain between the two red dots in the south of the island. Then, construction land extended to the southwest coastal plain, east shoreline reclamation area, and the southern islands. Finally, the construction land arrived at the north coastal plain and the north shoreline reclamation area. Correspondingly, the cropland/grassland distributed in the vast expanse in the coastal plain decreased and became discrete. The expansive cropland/grassland scattered among the plains and intermountain basins on the coast of Zhoushan Island in the preliminary stage of the study decreased rapidly after the expansion of construction land. As shown in the classification results in 2016, the cropland/grassland was mainly present in the northwest of the island, southwest coastal plains, and the interval basins at the end of this research. The overall spatial distribution tended to be discrete.

TABLE 5. Transition matrix of land-use type from 1984 to 2016.

2016 \ 1984	Construction land (km^2)	Forest (km^2)	Water body (km^2)	Cropland/ grassland (km^2)	Bare land (km^2)	Mudflat (km^2)	Seawater (km^2)	Total in 1984 (km^2)
Construction land	15.47	3.65	0.65	60.42	2.07	19.28	29.88	131.42
Forest	0.09	192.22	0.14	26.23	7.85	0.03	0.22	226.78
Water body	0.06	0.13	4.23	1.67	0.09	0.36	4.64	11.18
Cropland/grassland	3.25	13.38	0.48	124.69	8.80	5.29	3.15	159.04
Bare land	0.66	1.33	0.13	7.45	1.02	3.15	6.54	20.28
Mudflat	0.01	0	0	0.17	0	0.91	0.85	1.94
Seawater	0.02	0	0	0.07	0.02	0.33	581.70	582.14
Total in 2016	19.56	210.71	5.63	220.70	19.84	29.35	626.98	/

Note: Numbers in the above table refer to the mutual transition area of various land use types, row number refers to the roll-in

(2) Forest spatial distribution changed a little, but bare land changed a lot. Forests account for the highest proportion in all of the land featured in the study area, above 40%, and forests are prevalent in the central hills and mountains on every island. Due to the large slope, it is difficult and costly to develop the forest; therefore, it was well protected; hence, the spatial distribution of the forest changed little. Bare land, however, is usually regarded as a transition of land-use function; therefore, the spatial distribution changed a lot. In the early part of the period of 1984–2016, bare land mostly located in the hills and intermountain basins, and in the late part of the period, bare land was mainly in the plains and coastal area following the forest planting and various construction projects implementation.

(3) In the coastal areas, the mudflat area was decreasing and the water body was increasing. In early research, there were lots of mudflats in the north coasts of Zhoushan Island and surrounding islands in the north of the research area; yet, the area of mudflat decreased sharply after 32 years of reclamation and development. At present, the small remaining mudflat areas are mainly located in the northwest of Zhoushan Island and west of Xiaogan Island.

In general, water resources in the research area were deficient. Surface runoff was relatively little, water resources were mainly supplied by a reservoir of rainfall, and ''water body'' mainly refers to the reservoir water. In early research, the water body was mainly within the forest, and part of the reservoir was located in plains; but after 2011, some reclaimed land was converted into water body, and the water body increased in the northwestern and northeastern coastal area of Zhoushan Island following the speed-up of reclamation.

3) LAND TRANSITION ANALYSIS

a: TRANSITION AREA ANALYSIS OF LAND-USE TYPE

Based on overlay analysis, the land-use transition matrix from 1984 to 2016 is shown in Table 5. In this matrix, ''seawater'' refers to the sea outside of the boundary of the research area, which might contain in the boundary abstraction due to the influence of tides.

Table 5 shows that the areas of construction land and water body increased in the study area and cropland/grassland and mudflat decreased significantly. The key features of land-use transition in the study area include the following: cropland/grassland and mudflat were converted into construction land, cropland/grassland were converted to and from mudflat, and reclaimed sea area was converted into construction land, bare soil, and water body, the details of which are as follows:

(1) In total, 4.09 km^2 of the construction land was converted into cropland/grassland (79.46% for 3.25/4.09), bare land (16.14% for 0.66/4.09), and other land-use types (4.40% for 0.18/4.09). In 2016, 45.97% (60.42/131.42) of construction land came from converted cropland/grassland, 22.74% (29.88/131.42) from newly added land from reclamation, and 14.67% (19.28/131.42) from mudflat, showing that the expansion of construction land was achieved mainly by the conversion of cropland/grassland and reclamation.

(2) In total, 18.49 km^2 of the forest was converted into cropland/grassland (72.36% for 13.38/18.49), construction land (19.74% for 3.65/18.49), and other land-use types (7.90% for 1.46/18.49). About 34.56 km^2 of other land-use types were converted into forests, most of which come from cropland/grassland (75.90% for 26.23/34.56) and bare land (22.71% for 7.85/34.56).

(3) In total, 1.40 km^2 of the water body was converted into construction land (46.43% for 0.65/1.40), cropland/grassland (34.29% for 0.48/1.40), and other land-use types (19.29% for 0.27/1.40). In 2016, 41.50% (4.64/11.18) of the water body came from newly added land from reclamation, 14.94% (1.67/11.18) from cropland/grassland, and 3.22% (0.36/11.18) from mudflat. Thus, the extension of the water body was mainly a result of reclamation and conversion of cropland/grassland.

(4) In total, 96.01 km^2 of cropland/grassland was converted into construction land (62.93% for 60.42/96.01), forest (27.32% for 26.23/96.01), bare soil (7.76% for 7.45/96.01), and other land-use types (1.99% for 1.91/96.01). Also, 34.35 km^2 of other land types were converted into cropland/grassland, in which forest, bare soil, mudflat, construction land, and other land-use types accounted for 38.95%

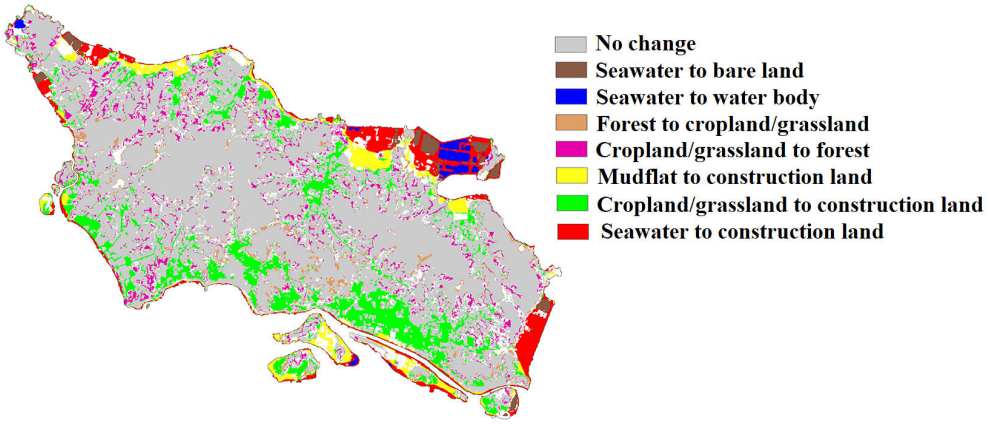

FIGURE 5. Spatial distribution of land transfer.

(13.38/34.35), 25.62% (8.80/34.35), 15.40% (5.29/34.35), 9.46% (3.25/34.35), and 10.57% (3.63/34.35) from newly added land from reclamation, respectively.

(5) About 28.44 km^2 of mudflat was converted into construction land (67.79% for 19.28/28.44), cropland/grassland (18.60% for 5.29/28.44), bare land (11.08% for 3.15/28.44), and other land-use types (3.52% for 0.72/28.44).

b: SPATIAL TRANSITION ANALYSIS OF LAND-USE TYPE

The critical spatial transition of land-use type is distributed, as shown in Fig 5. Because the hilly area on the island is difficult to develop, the land transition in the research area occurred mainly in the coastal area of the islands. The conversion of cropland/grassland into construction land occurred mainly in the south and north sea coast, central plains of Zhoushan Island, and coastal plains of other islands. It is greatest along the southern coast, which was the main distribution area of the conversion of cropland/grassland into construction land. The conversion of mudflat into construction land occurred in the seacoast of all the islands, but large-scale transition occurred mainly in the north of Zhoushan Island, Changzhi Island, Xiaogan Island, and Aoshan Island.

The most evident transition between cropland/grassland and the forest was the marginal area of hills in Zhoushan Island. On the whole, the forest changes to cropland/grassland mainly occurred in the south of Zhoushan Island, while cropland/grassland changes to the forest mainly in the west of Zhoushan Island.

Seawater being transferred into construction land and bare soil occurred mainly in east, northeast, and northwest of Zhoushan Island. The seawater was converted into inland water body located in the northeast and northwest of Zhoushan Island and the southeast of Changzhi Island.

4) RECLAMATION ANALYSIS

The land area of the city of Zhoushan is small, and the land resources are deficient, so reclamation is a crucial method by which to relieve the supply pressure on the land. By way of reclamation (including inning of mudflat and

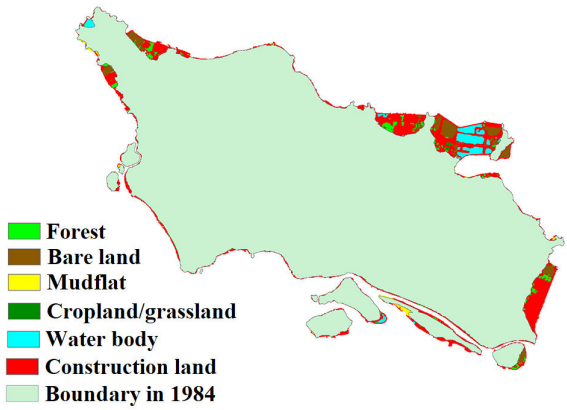

FIGURE 6. Location of reclaimed land from 1984 to 2016.

reclamation after siltation), mudflat in the research area has been converted into other land-use types, mainly construction land, and the seacoasts in each island have been extended toward the sea in various degrees. Within the 32-year period, the mudflat decreased by 93.39%, totaling 27.41 km^2; at the same time, the newly added land area increased by 8.87%, totaling 45.28 km^2, resulting in a total increase of the study area. The spatial distribution of newly added land by reclamation is shown in Fig. 6. Noticeable expansion of the seacoasts of the northwest, north, and east of Zhoushan Island and the southern islands in the study area occurred. As shown in Fig. 6, 65.99% of the newly added land was converted into construction land, 14.44% into bare soil, 10.25% into water body, and 6.96% into cropland/grassland; mudflat and forest accounted for 1.88% and 0.49%, respectively.

On the one hand, reclamation provides precious land sources for the construction development of Zhoushan, alleviating the local human–land conflicts and the problems of economic and social development caused by the lack of land resources in coastal areas. In turn, it promoted the rapid growth of the marine economy in the study area, as well as the promotion of urbanization, industrialization, and population agglomeration trends. On the other hand, the reclamation project has a significant impact on the marine ecological

environment and the nearshore hydrodynamic environment. Mudflats are habitats and breeding grounds of many species. Large-scale reclamation may lessen the coastal wetlands and destroy fish habitat and biodiversity. As one of China's four major fishing grounds, Zhoushan's large-scale reclamation project has caused local fishery resources to show signs of decline in recent years. To meet the needs of the construction of the Zhoushan Archipelago, many harbor industries have taken root in the longshore of the reclaimed area, and the manufacturing will inevitably result in nearshore water pollution of varying degrees. The reclaiming project will also change the dynamic water conditions of nearshore areas, such as the tides and waves, and then, it will affect the sediment transport pattern and change the seacoast scouring and siltation tendency.

V. CONCLUSION

Based on the data source from Landsat multitemporal data, this study compared the land-use information of the Zhoushan Archipelago in seven periods over 32 years obtained using the supervised classification method. As shown in the study, (1) There were large forests in the research area, which have been protected well during the development of the city. In general, the total area slightly increased, but spatial distribution changed very little. (2) Construction land continued to increase, and it increased by 571.88% in total over 32 years. The construction land gradually expanded to all of the coastal plains and southern islands with a trend ''first southward, then eastward, and finally northward'' from two centers of the southern plains of Zhoushan Island, using conversion of cropland/grassland and reclamation from the sea. (3) The large pieces of cropland/grassland spread across the coastal plains and intermountain basins were gradually occupied following the expansion of construction land, and the cropland/grassland decreased by 27.94% overall. The existing cropland/grassland mainly located in the western half of the seashore plains of Zhoushan Island and the central intermountain basins, and the spatial distribution was determined to be discrete. As the quantity of cropland/grassland decreased, the spatial distribution became more non-uniform. (4) After reclamation, the mudflat decreased by 93.35%, and most of it was converted into construction land. Meantime, newly added land totaled 45.28 km^2, and the total research area increased by 8.87%. Reclamation from the sea is the key method of city expansion and spatial development of Zhoushan Archipelago, but doing so results in a huge negative influence on coastal ecology and the environment.

It needs to be mentioned that this research is still limited to the image resolution and surface features within the research area, the cropland and grassland cannot be isolated, and the classification accuracy of the margin of sea and land is quite low. Also, since an in-depth discussion of the influence of land-use change on the regional environment and socially productive activities was not included, further study is needed.

ACKNOWLEDGMENT

The authors would like to thank the editors and the anonymous reviewers for their outstanding comments and suggestions, which greatly helped them to improve the technical quality and presentation of the manuscript. They also greatly appreciate the USGS (https://www.usgs.gov) and Geospatial Data Cloud (http://www.gscloud.cn) for the free availability of Landsat remotely-sensed image.

They also thank LetPub (www.letpub.com) for its linguistic assistance during the preparation of this manuscript.

REFERENCES

[1] D. Zhou, S. Zhao, L. Zhang, and S. Liu, ''Remotely sensed assessment of urbanization effects on vegetation phenology in China's 32 major cities,'' *Remote Sens. Environ.*, vol. 176, pp. 272–281, Apr. 2016.

[2] P. Gong, X. Li, and W. Zhang, ''40-Year (1978–2017) human settlement changes in China reflected by impervious surfaces from satellite remote sensing,'' *Sci. Bull.*, vol. 64, no. 11, pp. 756–763, Jun. 2019.

[3] B. M. Sleeter, J. Liu, C. Daniel, B. Rayfield, J. Sherba, T. J. Hawbaker, Z. Zhu, P. C. Selmants, and T. R. Loveland, ''Effects of contemporary land-use and land-cover change on the carbon balance of terrestrial ecosystems in the united states,'' *Environ. Res. Lett.*, vol. 13, no. 4, Mar. 2018, Art. no. 045006.

[4] C. Chen, J. Q. Fu, X. X. Sui, X. Lu, and A. H. Tan, ''Construction and application of knowledge decision tree after a disaster for water body information extraction from remote sensing images,'' *J. Remote Sens.*, vol. 22, no. 5, pp. 792–801, Sep. 2018.

[5] M. Kakooei and Y. Baleghi, ''A two-level fusion for building irregularity detection in post-disaster VHR oblique images,'' *Earth Sci. Informat.*, vol. 13, no. 2, pp. 459–477, Feb. 2020.

[6] C. Chen, J. Fu, S. Zhang, and X. Zhao, ''Coastline information extraction based on the tasseled cap transformation of Landsat-8 OLI images,'' *Estuarine, Coastal Shelf Sci.*, vol. 217, pp. 281–291, Feb. 2019.

[7] J. Chen, D. Pan, Z. Mao, N. Chen, J. Zhao, and M. Liu, ''Land-cover reconstruction and change analysis using multisource remotely sensed imageries in Zhoushan Islands Since 1970,'' *J. Coastal Res.*, vol. 294, pp. 272–282, Mar. 2014.

[8] U. Shafi, R. Mumtaz, N. Iqbal, S. M. H. Zaidi, S. A. R. Zaidi, I. Hussain, and Z. Mahmood, ''A multi-modal approach for crop health mapping using low altitude remote sensing, Internet of Things (IoT) and machine learning,'' *IEEE Access*, vol. 8, pp. 112708–112724, 2020.

[9] Q. Sun, P. Zhang, D. Sun, A. Liu, and J. Dai, ''Desert vegetation-habitat complexes mapping using Gaofen-1 WFV (wide field of view) time series images in Minqin County, China,'' *Int. J. Appl. Earth Observ. Geoinf.*, vol. 73, pp. 522–534, Dec. 2018.

[10] L. Xu, W. Jing, H. Song, and G. Chen, ''High-resolution remote sensing image change detection combined with pixel-level and object-level,'' *IEEE Access*, vol. 7, pp. 78909–78918, 2019.

[11] E. H. Wilson and S. A. Sader, ''Detection of forest harvest type using multiple dates of landsat TM imagery,'' *Remote Sens. Environ.*, vol. 80, no. 3, pp. 385–396, Jun. 2002.

[12] P. R. Sethre, B. C. Rundquist, and P. E. Todhunter, ''Remote detection of prairie pothole ponds in the Devils Lake Basin, North Dakota,'' *GISci. Remote Sens.*, vol. 42, no. 4, pp. 277–296, Dec. 2005.

[13] M. H. Mokhtari, K. Deilami, and V. Moosavi, ''Spectral enhancement of landsat OLI images by using hyperion data: A comparison between multilayer perceptron and radial basis function networks,'' *Earth Sci. Informat.*, vol. 13, no. 2, pp. 493–507, Jun. 2020.

[14] I. R. Orimoloye, S. P. Mazinyo, A. M. Kalumba, W. Nel, A. I. Adigun, and O. O. Ololade, ''Wetland shift monitoring using remote sensing and GIS techniques: Landscape dynamics and its implications on Isimangaliso Wetland Park, South Africa,'' *Earth Sci. Informat.*, vol. 12, no. 4, pp. 553–563, Aug. 2019.

[15] K. Liu, H. Su, X. Li, W. Wang, L. Yang, and H. Liang, ''Quantifying spatial–temporal pattern of urban heat Island in Beijing: An improved assessment using land surface temperature (LST) time series observations From LANDSAT, MODIS, and Chinese new satellite GaoFen-1,'' *IEEE J. Sel. Topics Appl. Earth Observ. Remote Sens.*, vol. 9, no. 5, pp. 2028–2042, May 2016.

[16] U. A. Bhatti, Z. Yu, L. Yuan, Z. Zeeshan, S. A. Nawaz, M. Bhatti, A. Mehmood, Q. U. Ain, and L. Wen, "Geometric algebra applications in geospatial artificial intelligence and remote sensing image processing," *IEEE Access*, vol. 8, pp. 155783–155796, 2020.
[17] Y. Chen, D. Ming, and X. Lv, "Superpixel based land cover classification of VHR satellite image combining multi-scale CNN and scale parameter estimation," *Earth Sci. Informat.*, vol. 12, no. 3, pp. 341–363, Apr. 2019.
[18] W. Sun, G. Yang, J. Peng, and Q. Du, "Lateral-slice sparse tensor robust principal component analysis for hyperspectral image classification," *IEEE Geosci. Remote Sens. Lett.*, vol. 17, no. 1, pp. 107–111, Jan. 2020.
[19] L. Xu, Y. Chen, J. Pan, and A. Gao, "Multi-structure joint decision-making approach for land use classification of high-resolution remote sensing images based on CNNs," *IEEE Access*, vol. 8, pp. 42848–42863, 2020.
[20] J. Q. Fu, C. Chen, and Y. L. Chu, "Spatial–temporal variations of oceanographic parameters in the Zhoushan sea area of the East China Sea based on remote sensing datasets," *Regional Stud. Mar. Sci.*, vol. 28, Apr. 2019, Art. no. 100626.
[21] W. Li, H. Liu, Y. Wang, Z. Li, Y. Jia, and G. Gui, "Deep learning-based classification methods for remote sensing images in urban built-up areas," *IEEE Access*, vol. 7, pp. 36274–36284, 2019.
[22] A. S. Rogers and M. S. Kearney, "Reducing signature variability in unmixing coastal marsh thematic mapper scenes using spectral indices," *Int. J. Remote Sens.*, vol. 25, no. 12, pp. 2317–2335, Jun. 2004.
[23] H. Singh, R. D. Garg, and H. C. Karnatak, "Online image classification and analysis using OGC Web processing service," *Earth Sci. Informat.*, vol. 12, no. 3, pp. 307–317, Feb. 2019.
[24] Z. Lv, T. Liu, C. Shi, J. A. Benediktsson, and H. Du, "Novel land cover change detection method based on k-Means clustering and adaptive majority voting using bitemporal remote sensing images," *IEEE Access*, vol. 7, pp. 34425–34437, 2019.
[25] W. Sun, J. Peng, G. Yang, and Q. Du, "Correntropy-based sparse spectral clustering for hyperspectral band selection," *IEEE Geosci. Remote Sens. Lett.*, vol. 17, no. 3, pp. 484–488, Mar. 2020.
[26] B. Guo, W. Zang, and R. Zhang, "Soil salizanation information in the Yellow River Delta based on feature surface models using Landsat 8 OLI data," *IEEE Access*, vol. 8, pp. 94303–94394, 2020.

CHAO CHEN (Associate Member, IEEE) received the B.E. degree in communication engineering and the M.S. degree in photogrammetry and remote sensing from the Shandong University of Science and Technology, Qingdao, China, in 2005 and 2009, respectively, and the Ph.D. degree in cartography and geography information system from Peking University, Beijing, China, in 2013. He is currently an Associate Professor with Zhejiang Ocean University, Zhoushan, China. His research interests include remote sensing image analysis and remote sensing of coastal environment.

HUIXIN CHEN received the B.S. degree in geographical science from the Guangdong University of Petrochemical Technology, Maoming, China, in 2020. She is currently pursuing the M.S. degree with Zhejiang Ocean University. Her research interest includes remote sensing image analysis. Her supervisor is Dr. Chao Chen.

WEIMIN LIAO received the B.S. degree in environmental science from Zhejiang Ocean University, Zhoushan, China, in 2011. He is currently an Engineer with the Zhoushan Natural Resources Surveying and Mapping Design Centre, Zhoushan. He mainly works on island survey, demonstration of sea area use, and environmental assessment of marine engineering.

XINXIN SUI received the B.E. degree in automation specialty from the North China University of Technology, Beijing, China, in 2003, and the M.S. degree in software engineering and the Ph.D. degree in cartography and geography information system from Peking University, Beijing, in 2006 and 2011, respectively. She is currently a Senior Engineer with the Land Satellite Remote Sensing Application Center, Ministry of Natural Resources, Beijing. She mainly works on mass remote sensing image processing and quality inspection.

LIYAN WANG received the B.S. degree in geographical science from Chuzhou University, Chuzhou, China, in 2020. She is currently pursuing the M.S. degree with Zhejiang Ocean University. Her research interest includes remote sensing image analysis. Her supervisor is Dr. Chao Chen.

JIANYU CHEN received the M.S. degree in environmental science and the Ph.D. degree in earth science from Zhejiang University, Hangzhou, China, in 1998 and 2004, respectively. He is currently a Professor of remote sensing with the State Key Laboratory of Satellite Ocean Environment Dynamics, Second Institute of Oceanography, Ministry of Natural Resources, Hangzhou. He has been a Postdoctoral Researcher with the Shanghai Institute of Technical Physics, Chinese Academy of Sciences, Shanghai, China. He has also been a Visiting Professor with the Department of Geography and Environmental Management, University of Waterloo, Waterloo, ON, Canada. His research interests include object-based image analysis, remote sensing of coastal environment, and geographic information systems.

YANLI CHU received the B.A. degree in art design from Zaozhuang University, Zaozhuang, China, in 2010, and the M.E. degree in industrial design from Guizhou Normal University, Guiyang, China, in 2014. Her main research interest includes information management.